# NYTEFOX 2020
# documentation Version v1.1

May 2021

Huss, Jannis-Michael; Zeller, Marie-Louise; Pfister, Lena; Lapo, Karl E.; Littmann, Daniela; Schneider, Johann; Schulz, Alexander; Thomas, Christoph K.

## Contents

## Setup (78.9ºN, 11.9 ºE)

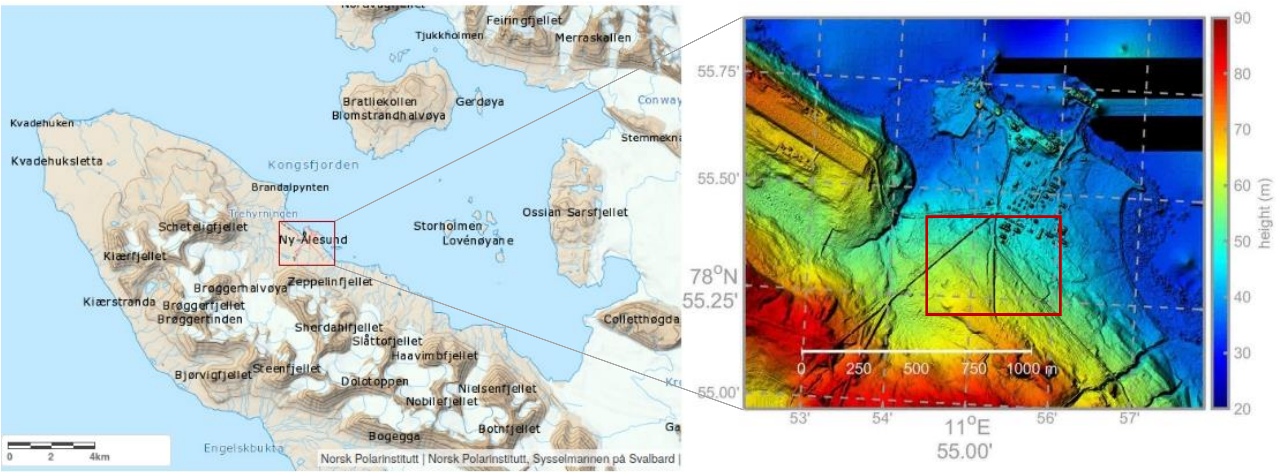


Figure 1. Left: Location Ny-Ålesund in the Kongsfjord from toposvalbard.npolar.no. Right: visualization of a digital elevation model published by Boike et al. (2018) around the location of the setup. The red frame marks the margins of Figure 2.


Figure 2. Setup south of Ny-Ålesund. The labels are the section names of the fiber optic Array (see *File overview*). The letters a-i mark crucial points with their coordinates listed in table 1. The map source is Svalbardkartet (geokart.npolar.no/Html5Viewer/index.html?viewer=Svalbardkartet).

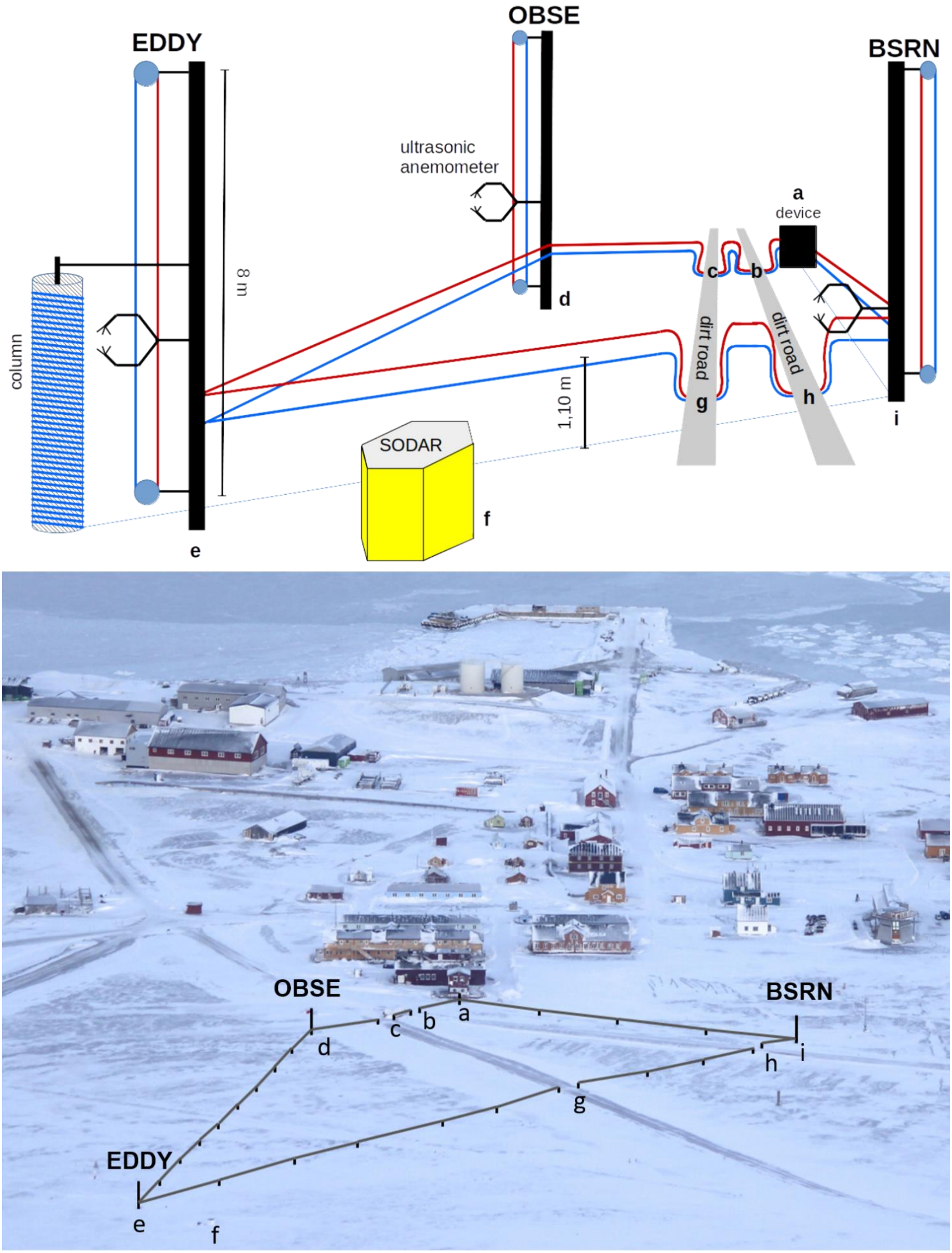


Figure 3. Schematic setup and picture of the setup from the Zeppelin mountain from south. The fiber-optic array has a length of 700 m. The coordinates of the characteristic points a-i of the schematic setup can be found in the Table 1. Photo credit: Harald Sodemann (UBergen, Norway).

Table 1. Setup locations, referenced in Figure 2 and 3, with corresponding coordinates. The uncertainty of the coordinates amounts 4 m.

| location name | location on map | latitude (°) | longitude (°) |
|---|---|---|---|
| Device in Ballon House | a | 78.92310 | 11.91811 |
| Crossing 1 | b | 78.92280 | 11.92122 |
| Crossing 2 | c | 78.92273 | 11.92063 |
| OBSE tower | d | 78.92266 | 11.91936 |
| EDDY tower | e | 78.92098 | 11.91382 |
| miniSODAR | f | 78.92082 | 11.91415 |
| Crossing 3 | g | 78.92171 | 11.92090 |
| Crossing 4 | h | 78.92207 | 11.92440 |
| BSRN tower | i | 78.92214 | 11.92508 |

# File overview

- Fiber Optic Distributed Sensing (FODS) data, all data were processed using the pyfocs library (Lapo & Freundorfer, 2020):
  - Horizontal and vertical fiber optic temperature measurements of unheated and heated fiber optic cables with a resolution of 0.127 m and 9 s
    - `NF_steel_[yyyymmdd]_cold.nc` (unheated measurements)
    - `NF_steel_[yyyymmdd]_warm.nc` (heated measurements)
      - daily netcdf files, containing the following variables:

| variable | Explanation | unit | dimension |
|---|---|---|---|
| LAF | Length along the fiber | m | xyz |
| x | Easting in UTM 33X | m | xyz |
| y | Northing in UTM 33X | m | xyz |
| z | Height above surface | m | xyz |
| cold/warm | String with names of the various fiber sections (named 'cold' for unheated, 'warm' for heated fiber) | - | xyz |
| time | Start time of aggregation interval (UTC) | seconds since first reading of the file | time |
| cal_temp | Calibrated temperatures | °C | time, xyz |

- Vertical high-resolution fiber optic temperature measurements from 0 to 2.5 m agl. with a temporal resolution of 9 s and a spatial resolution along the fiber of 0.25 m. Note that the effective vertical resolution ranges from 0.0025 to 0.02 m due to helically coil-wrapping the fiber optic cable (see Sigmund et al., 2017):
  - `NF_column.rar`
    - RAR-archive, containing 14 netcdf files of one day each
      - `NF_column_eddy_[yyyymmdd].nc`
        variables: same as above

- Ultrasonic anemometers
  - Turbulence measurements with ultrasonic anemometers, mounted at three towers (OBSE, EDDY, BSRN), raw (20 Hz) data were processed using the bmmflux software (see Thomas et al., 2009, Appendix for processing)
  - `NF_sonic_OBSE.rar`
  - `NF_sonic_EDDY.rar`
  - `NF_sonic_BSRN.rar`
    - mounting parameters:

| | azimuth (°) | height (m) | distance from mast (m) |
|---|---|---|---|
| OBSE | 203 | 1.48 | 0.77 |
| EDDY | 201 | 1.35 | 0.80 |
| BSRN | 208 | 1.50 | 0.91 |

    - RAR-archives, containing ‘results’ and ‘qaqc’ files as CSV for two perturbation time scales (30 s and 2 min, example for OBSE tower):
      - `Nytefox2020_OBSE-EC_results_1p57m_30s_rot_frc.csv`
      - `Nytefox2020_OBSE-EC_qaqc_1p57m_30s_rot_frc.csv`
      - `Nytefox2020_OBSE-EC_results_1p57m_2min_rot_frc_tom.csv`
      - `Nytefox2020_OBSE-EC_qaqc_1p57m_2min_rot_frc_tom.csv`
      - third order moments are only computed for the 2 min perturbation time scale
        - a list of output statistics is given in:
          `NF_sonic_output_explanation.pdf`

- miniSodar
  - ground-based acoustic remote sensing measurements, using SOund Detection And Ranging (SODAR): vertical measurements of horizontal wind speed and direction, vertical velocity variance, backscatter intensity, and turbulence kinetic energy from 10 up to 300 m agl. with a resolution of 5 m vertically and averaged over 10 min.
  - `NF_miniSODAR.rar`
    - RAR-archive, containing daily netcdf files:
      - `NYTEFOX2020_MiniSodar_ProcessedData_[yyyy-mm-dd].nc`
      - azimuth: 356°

- variables:

| variable | explanation | unit | aggregation | dimension |
|---|---|---|---|---|
| z | Center height of vertical gate | m agl. | 5 m | height |
| SPD | Horizontal wind speed | m $s^{-1}$ | 5 m and 10 min | time, height |
| DIR | Horizontal wind direction | ° | 5 m and 10 min | time, height |
| u | Meridional wind speed component (positive from West to East) | m $s^{-1}$ | 5 m and 10 min | time, height |
| v | Zonal wind speed component (positive from South to North) | m $s^{-1}$ | 5 m and 10 min | time, height |
| w | Vertical wind speed component (positive for updrafts, negative for downdrafts) | m $s^{-1}$ | 5 m and 10 min | time, height |
| sigmaw | Standard deviation of the vertical wind speed component | m $s^{-1}$ | 5 m and 10 min | time, height |
| r | Acoustic reflectivity (Raw Backscatter Intensity) | dB | 5 m and 10 min | time, height |
| TKE | Turbulence Kinetic Energy | $m^2$ $s^{-2}$ | 5 m and 10 min | time, height |
| time | Start time of aggregation intervals | Matlab serial format: days since Jan 00, 0000 | | time |

## Data availability

The data availability from all observational systems for the campaign period in February and March 2020 is summarized in Figure 4. Gaps in records were caused by instrument failure and post-field data processing.
The FODS data files containing actively heated fiber temperatures (used for wind speed computations) include data from a period when heating was working only intermittently or at non-optimal heating rates (start to 27.02.2020, 18:44 UTC). After 27.02.2020 at 18:45 UTC all heating issues were resolved and this period offers the best data quality (as indicated in Figure 4).

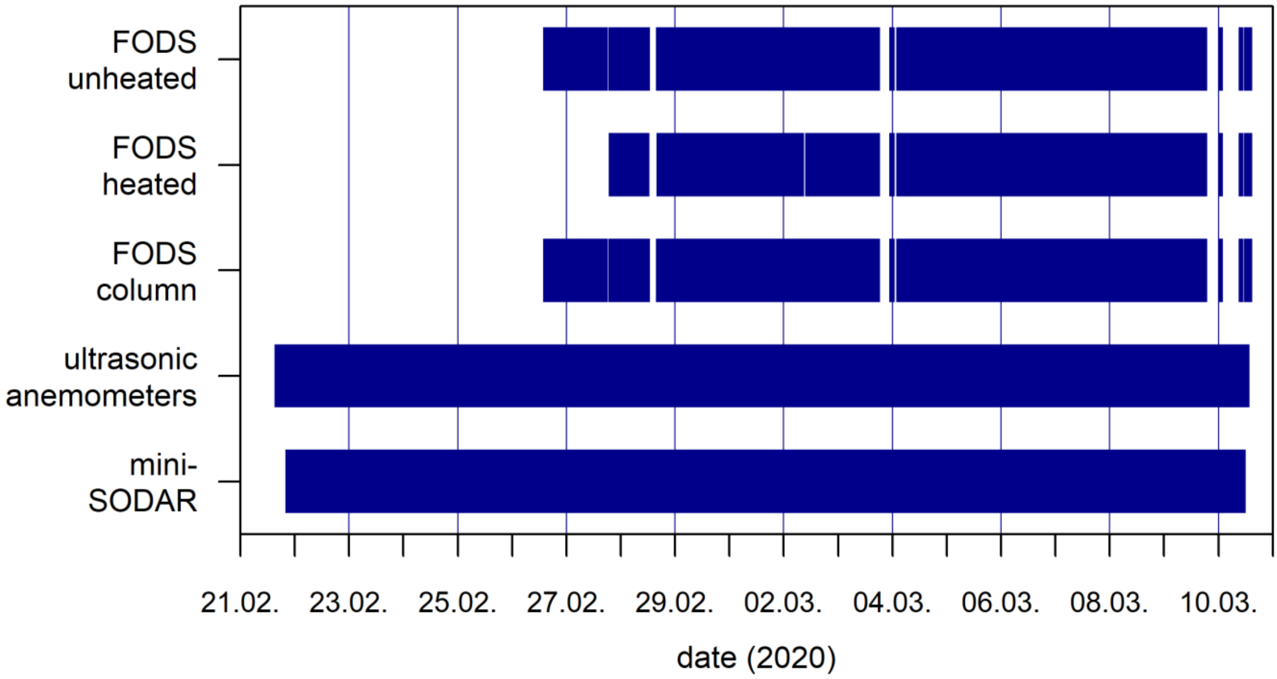


Figure 4: Data availability of the different data sets of NYTEFOX for the campaign period in February and March 2020. Gaps in the FODS data sets occur due to instrument and calibration failures.

# References

Boike, J., Juszak, I., Lange, S., Chadburn, S., Burke, E. J., Overduin, P. P., Roth, K., Ippisch, O., Bornemann, N., Stern, L., Gouttevin, I., Hauber, E., and Westermann, S.: HRSC-AX data products (DEM and multi channel) from aerial overflights in 2008 over Bayelva (Brøggerhalvøya peninsula, Spitsbergen), PANGAEA, https://doi.org/10.1594/PANGAEA.884730, in supplement to: Boike, J et al. (2018): A 20-year record (1998-2017) of permafrost, active layer and meteorological conditions at a high Arctic permafrost research site (Bayelva, Spitsbergen). Earth System Science Data, 10(1), 355-390, https://doi.org/10.5194/essd-10-355-2018, 2018.

Lapo, K. and Freundorfer, A.: pyfocs v0.5, Zenodo, https://doi.org/10.5281/zenodo.4292491, https://github.com/klapo/pyfocs, 2020.

Sigmund, A., Pfister, L., Sayde, C., and Thomas, C. K.: Quantitative analysis of the radiation error for aerial coiled-fiber-optic distributed temperature sensing deployments using reinforcing fabric as support structure, Atmospheric Measurement Techniques, 10, 2149–2162, https://doi.org/10.5194/amt-10-2149-2017, https://www.atmos-meas-tech.net/10/2149/2017/, 2017.

Thomas, C., Law, B., Irvine, J., Martin, J., Pettijohn, J., and Davis, K.: Seasonal hydrology explains interannual and seasonal variation in carbon and water exchange in a semiarid mature ponderosa pine forest in central Oregon, Journal of Geophysical Research: Biogeosciences, 114, https://doi.org/10.1029/2009JG001010, 2009.